Influence of lithium content on high rate cycleability of layered $Li_{1+x}Ni_{0.30}Co_{0.30}Mn_{0.40}O_2$ cathodes for high power lithium-ion batteries

R. Santhanam, Philip Jones, Adusumilli Sumana, B. Rambabu *

Solid State Ionics and Surface Sciences Lab, Department of Physics, Southern University and A&M College, Baton Rouge, LA 70813, USA

ARTICLE INFO

ABSTRACT

Layered $Li_{1+x}Ni_{0.30}Co_{0.30}Mn_{0.40}O_2$ ($x = 0$, 0.05, 0.10, 0.15) materials have been synthesized using citric acid assisted sol–gel method. The materials with excess lithium showed distinct differences in the structure and the charge and discharge characteristics. The rate capability tests were performed and compared on $Li_{1+x}Ni_{0.30}Co_{0.30}Mn_{0.40}O_2$ ($x = 0$, 0.05, 0.10, 0.15) cathode materials. Among these materials, $Li_{1.10}Ni_{0.30}Co_{0.30}Mn_{0.40}O_2$ cathode demonstrated higher discharge capacity than that of the other cathodes. Upon extended cycling at 1C and 8C, $Li_{1.10}Ni_{0.30}Co_{0.30}Mn_{0.40}O_2$ showed better capacity retention when compared to other materials with different lithium content. $Li_{1.10}Ni_{0.30}Co_{0.30}Mn_{0.40}O_2$ exhibited 93 and 90% capacity retention where as $Li_{1.05}Ni_{0.30}Co_{0.30}Mn_{0.40}O_2$, $Li_{1.15}Ni_{0.30}Co_{0.30}Mn_{0.40}O_2$, and $Li_{1.00}Ni_{0.30}Co_{0.30}Mn_{0.40}O_2$ exhibited only 84, 71, and 63% (at 1C), and 79, 66 and 40% (at 10C) capacity retention, respectively, after 40 cycles. The enhanced high rate cycleability of $Li_{1.10}Ni_{0.30}Co_{0.30}Mn_{0.40}O_2$ cathode is attributed to the improved structural stability due to the formation of appropriate amount of Li_2MnO_3-like domains in the transition metal layer and decreased Li/Ni disorder (i.e., Ni content in the Li layer).

1. Introduction

Lithium-ion batteries have revolutionized consumer electronic devices and become dominant power sources for cell phones, camcorders and lap-top computers, etc. due to their light weight, high energy density, long cycle life [1–4]. However, present lithium-ion technologies fall short of meeting the higher charge–discharge rate capability requirement of hybrid, plug-in hybrid and full electric vehicles, which was considered to relieve side issues linked to air pollution combined with the foreseen oil shortage. Since the demand for high performance exceeds the capabilities of the existing lithium-ion battery technology, electrode materials with excellent electrochemical performance and low cost must be developed. Researchers at Sony Corporation developed the first commercial lithium-ion batteries in 1990, using $LiCoO_2$ as a cathode, and this material continues to be used in more than 90% of lithium-ion batteries manufactured despite the high cost and safety hazards associated with cobalt [5,6]. A variety of efforts have been undertaken over the past decade to find possible alternatives to $LiCoO_2$ in lithium-ion batteries. In recent years, the lithium transition metal oxides, $Li[Ni_xCo_{1-2x}Mn_x]O_2$ have received considerable interest as a candidate to replace the commercial $LiCoO_2$ cathode material for lithium secondary batteries [7–10]. Among them, $LiNi_{1/3}Co_{1/3}Mn_{1/3}O_2$ and modified $LiNi_{1/3}Co_{1/3}Mn_{1/3}O_2$ materials have been studied extensively as a promising cathode material due to its many advantages such as a high discharge capacity, high rate capability, and good structural stability [11–17]. It has been reported that the $LiNi_{1/3}Co_{1/3}Mn_{1/3}O_2$ material could deliver reversible capacity of 160 and 200 mAh g^{-1} in the voltage range of 2.5–4.4 and 2.8–4.6 V, respectively [18,19].

In order to further enhance $LiNi_{1/3}Co_{1/3}Mn_{1/3}O_2$ material's electrochemical properties, many studies have been carried out to improve the performance of this active material by cationic substitution. It is generally known that doping of electrochemically inactive metals such as Mg, Nb, Si, and Zr in the $LiNi_{1/3}Co_{1/3}Mn_{1/3}O_2$ would improve electrochemical and thermal stabilities. Hence, to improve the electrochemical properties, Na et al. [20] doped Si with $LiNi_{0.30}Co_{0.30}Mn_{0.40}O_2$ and found that the electrochemical properties such as capacity and cycle life were improved significantly. Al and Fe substituted $LiNi_{1/3}Co_{1/3}Mn_{1/3}O_2$ materials were prepared by firing coprecipitates of Ni, Co, Mn hydroxides by Liu et al. [21]. They reported that Fe substitution did not improve the electrochemical performance; however, doping of small amount of Al improved the capacity retention of $LiNi_{1/3}Co_{1/3}Mn_{1/3}O_2$ material. An alternate approach to improve electrochemical performance is to change the surface properties of the cathode material by coating its particle with some metal oxides to avoid the unwanted reactions on the surface and protect

* Corresponding author. Tel.: +1 225 771 4130; fax: +1 225 771 2310.
E-mail address: rambabu@cox.net (B. Rambabu).

the bulk. Recently, Hu et al. reported that the cycle life performance of $LiNi_{1/3}Co_{1/3}Mn_{1/3}O_2$ was improved by a ZrO_2 coating [22]. Similarly, other research groups reported that a metal oxide coating significantly improved the electrochemical properties of without significant specific capacity loss, and the metal oxide coating layer acted as solid electrolyte with a reasonable high Li ion conductivity [23,24]. Recently, Kang et al. studied the effect of lithium content on structure and electrochemical properties of battery cathode material, $LiNi_{0.5}Mn_{0.5}O_2$ [25]. They added excess lithium because they expected that the excess lithium would reside in the transition metal layers and form Li_2MnO_3-like phases which would affect the electronic and crystallographic structure of the $LiNi_{0.5}Mn_{0.5}O_2$ material. From the experimental results, Kang et al. [25] proved that the excess lithium significantly affected the discharge performance at the low voltage range and the rate capability of the material.

In the present work, lithium nickel cobalt manganese oxides with various lithium contents, i.e., $Li_{1+x}Ni_{0.30}Co_{0.30}Mn_{0.40}O_2$ ($x=0$, 0.05, 0.10, 0.15) have been prepared using citric acid assisted sol–gel method. The effects of lithium content on the crystal structure and the electrochemical properties such as rate capability and high rate cycleability are systematically studied and reported in this paper.

2. Experimental

$Li_{1+x}Ni_{0.30}Co_{0.30}Mn_{0.40}O_2$ cathode materials ($x=0$, 0.05, 0.10, 0.15) with different Li content were synthesized by the citric acid sol–gel method [26] in the following manner. Stoichiometric amounts of $Li(CH_3COO)\cdot2H_2O$, $Ni(CH_3COO)_2\cdot4H_2O$, $Co(CH_3COO)_2\cdot4H_2O$, and $Mn(CH_3COO)_2\cdot4H_2O$ were dissolved in distilled water. Citric acid was used as a chelating agent. The solution pH was adjusted to 7.0 with ammonium hydroxide. The solution was heated at 70–80 °C until a transparent sol was obtained. The resulting gel precursor was dried at 120 °C for 4 h in air and followed with decomposition at 450 °C for 8 h to remove the organic contents. The decomposed powders were ground by ball milling (Spex 8000 Mixer/Mill) with stainless steel balls for 2 h and sintered at 850 °C in air for 12 h. The heating and cooling rates of the powder were 4 °C and 2 °C min^{-1}, respectively.

Li, Co, Ni and Mn contents in the resulting materials were analyzed using an inductively coupled plasma/atomic emission spectrometer (ICP/AES). The measured composition of the materials is close to the target composition so that the nominal compositions are used to describe the materials throughout this paper for simplicity. The phase purity was verified from powder X-ray diffraction (XRD) measurements. The particle morphology of the powders after sintering was obtained using a scanning electron microscopy (SEM). The charge and discharge characteristics of cathodes were examined in a CR2032 coin type half-cell. Cells were composed of a cathode and a lithium metal anode separated by a porous polypropylene separator (Celgard). Composite cathode was prepared by thoroughly mixing the active material (80%) with Super P carbon (10%) and polyvinylidene fluoride (10%) in N-methyl-pyrrolidinone. The slurry was then cast on aluminum foil and dried at 90 °C for 10 h in vacuum. The resulting electrode film was subsequently pressed and punched into a circular disc. The electrolyte solution used was 1 M $LiPF_6$ in a mixture of ethylene carbonate–diethyl carbonate (1:1 volume, Ferro Corporation, USA). The coin cell was assembled in an argon-filled glove box (Vacuum Atmospheres, USA). The cells were cycled at different C-rates between 2.5 and 4.3 V with an Arbin battery testing system. The current value for different C-rates were calculated from the theoretical capacity of stoichiometric $LiNi_{0.3}Co_{0.3}Mn_{0.4}O_2$ (1C = 150 mAh g^{-1}).
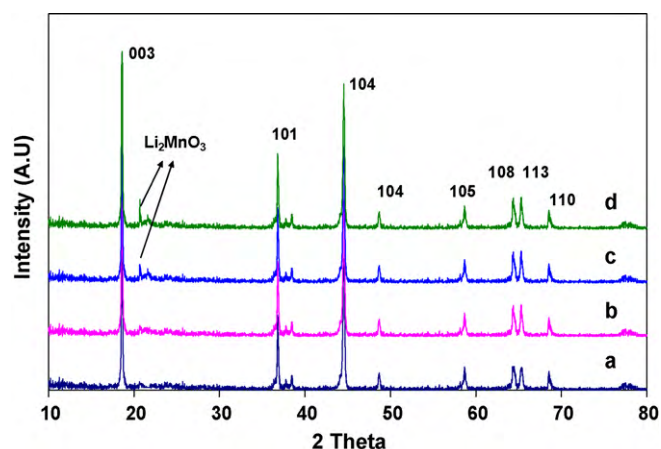
Fig. 1. XRD patterns of the $Li_{1+x}Ni_{0.30}Co_{0.30}Mn_{0.40}O_2$ with different Li contents. (a) $x=0.00$, (b) $x=0.05$, (c) $x=0.10$, and (d) $x=0.15$.

3. Results and discussion

Fig. 1 shows the powder XRD patterns of the $Li_{1+x}Ni_{0.30}Co_{0.30}Mn_{0.4}O_2$ ($x=0$, 0.05, 1.00, 1.15) materials. All the diffraction peaks can be indexed as a layered oxide structure based on a hexagonal α-NaFeO$_2$ structure with a space group R3-m. The small diffraction peaks at 20–25°$2\theta_{CuK\alpha}$ that are generally attributed to the cation ordering between Li and Ni/Co/Mn in the transition metal layer [27,28]. As can be seen in Fig. 1, those small cation ordering peaks become more distinctive with increasing lithium content (x). It has been reported that layered lithium-rich metal oxides form a composite structure consisting of monoclinic Li_2MnO_3 and hexagonal $LiMO_2$ phases (M = Ni, Co, Mn, etc.); the presence of Li_2MnO_3-like domains has been demonstrated by various experimental techniques including XRD [28–31]. Similarly, the $Li_{1+x}MO_2$ materials can be alternatively represented in a two-component "composite" notation as $xLi_2MnO_3\cdot(1-x)$ $LiMO_2$ (M = Ni, Co, Mn, etc.) to account for these domains. Recently, the structural aspects of lithium-rich $Li_{1+x}(Ni_{0.5}Mn_{0.5})_{1-x}O_2$ materials have been explained in detail by Thackeray et al. [32]. The layered oxide structure has lithium ions at the 3a, the transition metal ions (Ni, Co, Mn) at 3b and oxygen ions at 6c sites. Since the ionic radii of Li$^+$ (0.76 Å) and Ni^{2+} (0.69 Å) ions are similar, a partial disordering among the 3a and 3b sites is expected and it is called as "cation-mixing" [33]. It has been established that the cation-mixing deteriorates the electrochemical performance of the layered oxide materials. The integrated intensity ratio of the (003) to (104) lines (R) in the XRD patterns was shown to be a measurement of the cation mixing and a value of $R < 1.2$ is an indication of undesirable cation mixing [33]. The oxygen sublattice in the –NaFeO$_2$ type structure is considered as distorted from the fcc array in the direction of hexagonal c-axis. This distortion gives rise to a splitting of the lines assigned to the Miller indices (006, 102) and (108, 110) in the XRD patterns and these are characteristic to the layer structure. The ratio of the intensities of the (003) and (104) peaks of the prepared $Li_{1+x}Ni_{0.30}Co_{0.30}Mn_{0.4}O_2$ materials, with different lithium content where $x=0$, 0.05, 1.00, 1.15 are around 1.02, 1.19, 1.31, 1.22, respectively. These R values would have direct influence of the electrochemical performance. The narrow diffraction peaks of the pattern indicate the high crystallinity of the prepared $Li_{1+x}Ni_{0.30}Co_{0.30}Mn_{0.40}O_2$ powders. In XRD patterns, the peak splits of 006/102 and 018/110 are known to be an indicator of layered structure such as LiCoO$_2$ and LiNiO$_2$. As can be seen in Fig. 1, clear peak splits of 006/102 and 108/110 are observed, which indicate the highly ordered layered structure of the prepared $Li_{1+x}Ni_{0.30}Co_{0.30}Mn_{0.40}O_2$ mate-
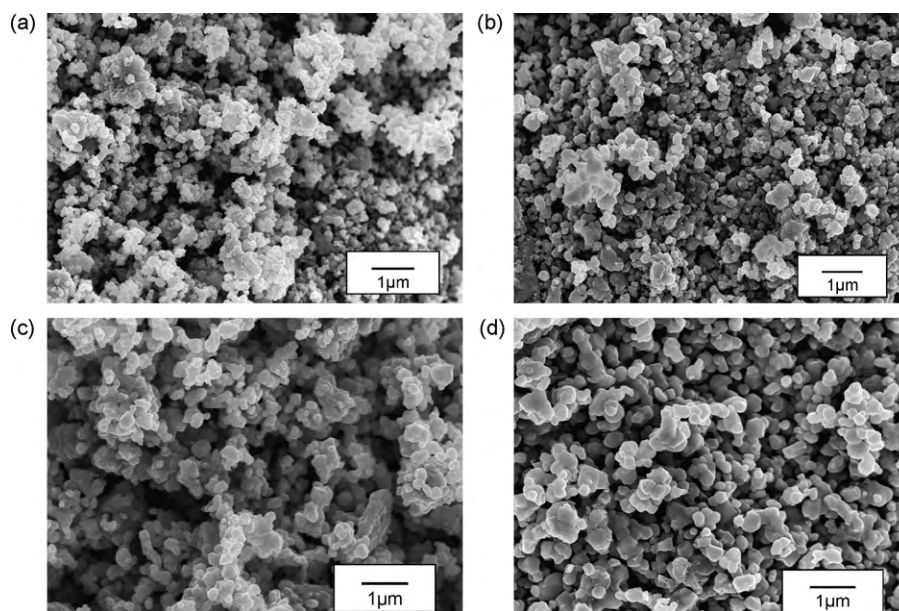
Fig. 2. SEM photographs of the $Li_{1+x}Ni_{0.30}Co_{0.30}Mn_{0.40}O_2$ with different Li contents. (a) $x = 0.00$, (b) $x = 0.05$, (c) $x = 0.10$, and (d) $x = 0.15$.

rials. It is known that the particle size, particle size distribution and morphology of the samples have a direct influence on the electrochemical performance of the electrode materials used in rechargeable lithium batteries. Fig. 2a–d shows SEM photographs of $Li_{1+x}Ni_{0.30}Co_{0.30}Mn_{0.4}O_2$ materials prepared by sol–gel method at the same sintering temperature of 850 °C with different lithium contents, $x = 0.00, 0.05, 1.00, 115$, respectively. It is noted that there exist distinct differences in the particle size depending on the lithium content. The materials with $x = 0.00$ and 0.05 show similar particle size and particle size distribution. However, the materials with higher lithium content ($x = 0.10, 0.15$) exhibit slightly larger particle size. The reason for the particle size differences presumably due to higher lithium content which enhances particle growth process. However, lithium content does not affect the morphology of the particle as can be seen from SEM images in Fig. 2a–d.

In order to evaluate the lithium content on the rate capability of $Li_{1+x}Ni_{0.30}Co_{0.30}Mn_{0.40}O_2$ ($x = 0.00, 0.05, 0.10, 0.15$) materials, the cells were cycled in the voltage range 2.5–4.3 V. Figs. 3–6 show the discharge capacities of the $Li_{1+x}Ni_{0.30}Co_{0.30}Mn_{0.40}O_2$/Li cells as a function of C-rate between 2.5 and 4.3 V vs Li. The cells were charged galvanostatically with a 0.1C-rate

before each discharge testing, and then discharged at different C-rates from 0.1 to 8C-rates (16–1280 mA g^{-1}). As can be clearly seen in Figs. 3–6, excess lithium clearly improves the rate capability, and the $Li_{1.10}Ni_{0.30}Co_{0.30}Mn_{0.4}O_2$ electrode (Fig. 5) delivered a higher capacity than the other electrodes $Li_{1.00}Ni_{0.30}Co_{0.30}Mn_{0.40}O_2$ (Fig. 3), $Li_{1.05}Ni_{0.30}Co_{0.30}Mn_{0.40}O_2$ (Fig. 4), and $Li_{1.15}Ni_{0.30}Co_{0.30}Mn_{0.40}O_2$ (Fig. 6) at different C-rates. For example, $Li_{1.10}Ni_{0.30}Co_{0.30}Mn_{0.40}O_2$ cathode delivered 158 mAh g^{-1}, however, the other electrodes $Li_{1.00}Ni_{0.30}Co_{0.30}Mn_{0.40}O_2$, $Li_{1.05}Ni_{0.30}Co_{0.30}Mn_{0.40}O_2$, and $Li_{1.15}Ni_{0.30}Co_{0.30}Mn_{0.40}O_2$ delivered only 147, 155 and 153 mAh g^{-1} at 0.1C. At 8C-rate, the obtained capacity retention of the $Li_{1.10}Ni_{0.30}Co_{0.30}Mn_{0.4}O_2$ was about 79%, compared to that of a 0.1C-rate, while the other electrodes showed capacity retention less than 79% at the same C-rate. The increase in specific discharge capacity of the material with appropriate amount of excess lithium might be attributed to the participation of Mn ions in the redox reactions. The discharge capacity values are shown in Table 1. It is also noted that the discharge voltage drop of the $Li_{1.10}Ni_{0.30}Co_{0.30}Mn_{0.40}O_2$ electrode during high rate discharge was much lower compared to the other three electrodes. The

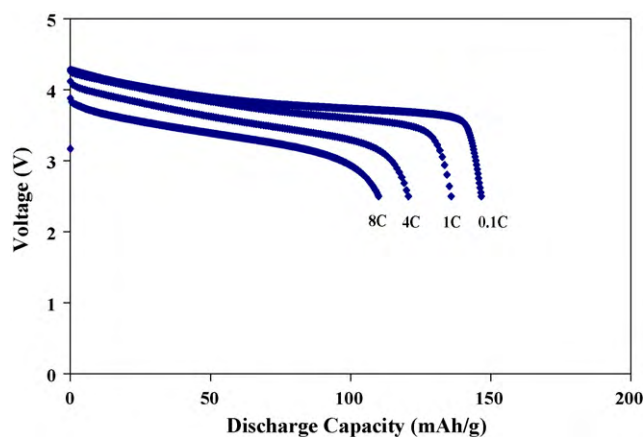**Fig. 3.** Initial discharge curves of $Li_{1.00}Ni_{0.30}Co_{0.30}Mn_{0.40}O_2$ electrode at different C-rates, 0.1, 1, 4, and 8C between 2.5 and 4.3 V.

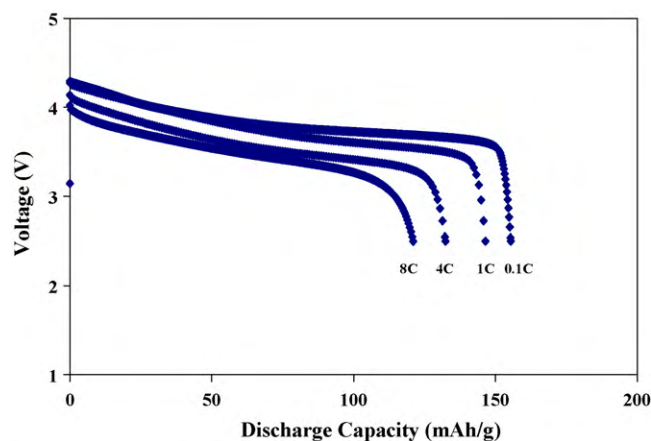**Fig. 4.** Initial discharge curves of $Li_{1.05}Ni_{0.30}Co_{0.30}Mn_{0.40}O_2$ electrode at different C-rates, 0.1, 1, 4, and 8C between 2.5 and 4.3 V.
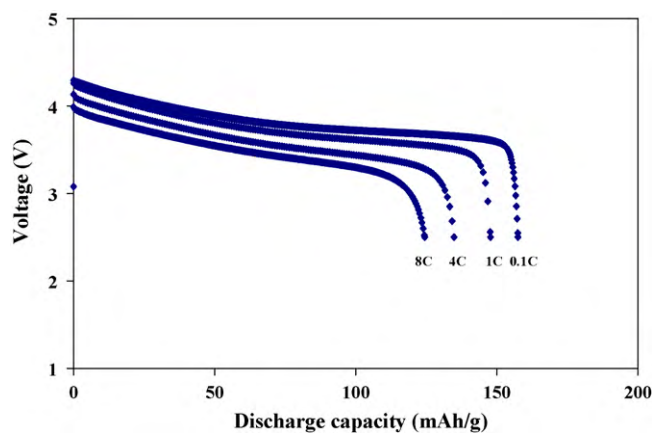
Fig. 5. Initial discharge curves of $Li_{1.10}Ni_{0.30}Co_{0.30}Mn_{0.40}O_2$ electrode at different C-rates, 0.1, 1, 4, and 8C between 2.5 and 4.3 V.

Table 1
Discharge capacities of cathode materials with different Li content at different C-rates.

Materials with different Li content	Discharge capacities at different C-rates, mAh g^{-1}			
	0.1C	1C	4C	8C
$Li_{1.00}Ni_{0.30}Co_{0.30}Mn_{0.40}O_2$	147	136	121	110
$Li_{1.05}Ni_{0.30}Co_{0.30}Mn_{0.40}O_2$	155	145	131	121
$Li_{1.10}Ni_{0.30}Co_{0.30}Mn_{0.40}O_2$	158	148	135	125
$Li_{1.15}Ni_{0.30}Co_{0.30}Mn_{0.40}O_2$	153	143	128	113

obtained results strongly supported that appropriate amount of excess lithium in $LiNi_{1/3}Co_{1/3}Mn_{1/3}O_2$ is very effective to enhance rate capability.

Fig. 7 compares the rate capability of the $Li/Li_{1+x}Ni_{0.30}Co_{0.30}Mn_{0.40}O_2$ cells in the voltage range of 2.8–4.3 V. For the rate capability study, each cell was charged to 4.3 V at 0.1C and then discharged to 2.5 V at various current rates 0.1, 1, 4 and 8C. As can be seen in Fig. 7, the rate capability was improved significantly with increasing appropriate amount of lithium. The highest rate capability was obtained for $x = 0.10$, followed by $x = 0.05$, 0.15, and then $x = 0$. In the literature, it was explained that $Li_{1.06}(Ni_{0.5}Mn_{0.5})_{0.94}O_2$ showed higher Li$^+$ diffusivity than $LiNi_{0.5}Mn_{0.5}O_2$, which was due to the reduced Ni content in the lithium layer in $Li_{1.06}(Ni_{0.5}Mn_{0.5})_{0.94}O_2$ [34]. Kang et al. were also reported that the rate capability of $LiNi_{0.5}Mn_{0.5}O_2$ was significantly
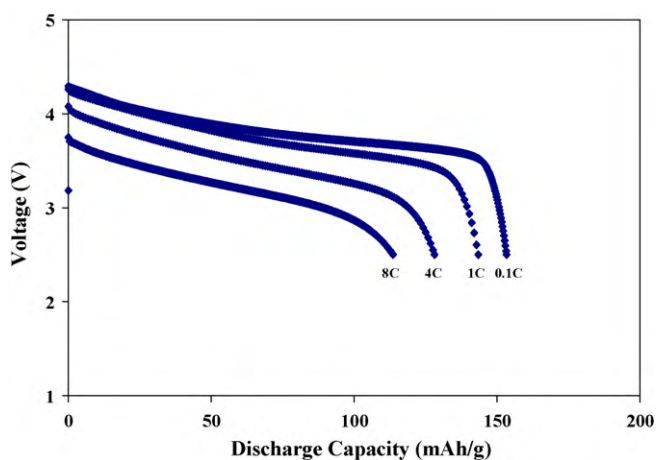

Fig. 7. Plot of % of discharge capacity vs C-rate of the $Li_{1+x}Ni_{0.30}Co_{0.30}Mn_{0.40}O_2$ materials with different Li content.

improved by reducing the extent of Li/Ni disorder in alternate layers of the structure [35]. From these results, we believe that the improved rate capability of the lithium-excess materials presented in this work is due to the reduced Ni content in the lithium layer as predicted from our XRD results.

In order to observe the influence of lithium content on cycling properties at high C-rates, $Li/Li_{1+x}Ni_{0.30}Co_{0.30}Mn_{0.40}O_2$ ($x = 0.00$, 0.05, 0.10, 0.15) cells were assembled and the performance was measured at 1 and 8C-rates between 2.5 and 4.3 V. Fig. 8a and b indicates that the cycling performance of $Li_{1.10}Ni_{0.30}Co_{0.30}Mn_{0.4}O_2$ electrode materials cycled at a high current rate of 1 and 8C, respectively. After 40 charge–discharge cycles at 1C, the $Li_{1.10}Ni_{0.30}Co_{0.30}Mn_{0.4}O_2$ electrode exhibits excellent cycling performance with capacity retention ratio of about 93% when compared to that of other electrodes $Li_{1.00}Ni_{0.30}Co_{0.30}Mn_{0.40}O_2$,

Fig. 8. High discharge rate cycling performance of $Li_{1+x}Ni_{0.30}Co_{0.30}Mn_{0.40}O_2$ electrode materials with different Li content at (a) 1C, and (b) 8C in the voltage range between 2.5 and 4.3 V.

Fig. 6. Initial discharge curves of $Li_{1.15}Ni_{0.30}Co_{0.30}Mn_{0.40}O_2$ electrode at different C-rates, 0.1, 1, 4, and 8C between 2.5 and 4.3 V.

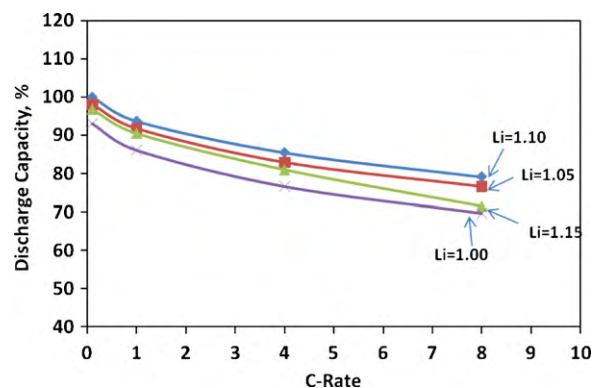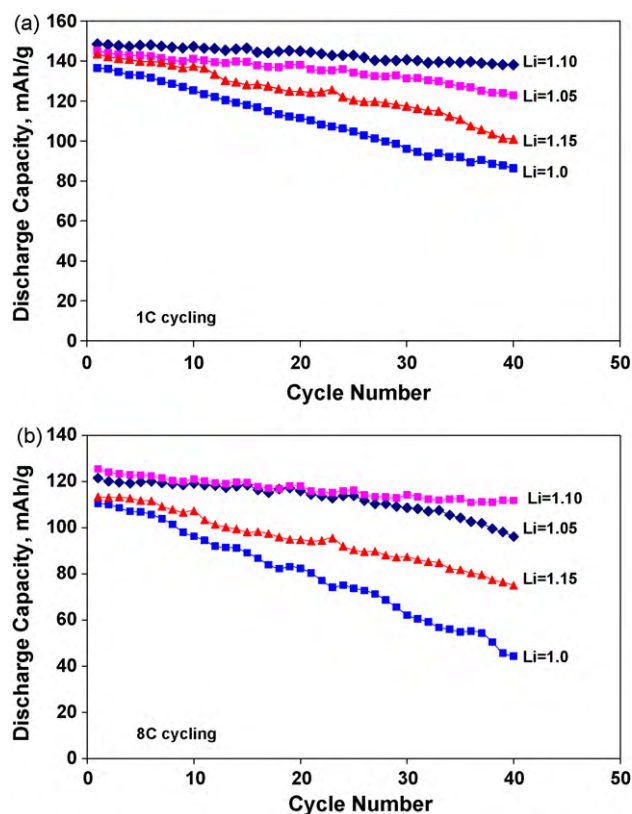$Li_{1.05}Ni_{0.30}Co_{0.30}Mn_{0.40}O_2$, and $Li_{1.15}Ni_{0.30}Co_{0.30}Mn_{0.40}O_2$ which show only 84, 71, and 63% capacity retention ratio, respectively. Similarly, after 40 charge–discharge cycles at high C-rate of 8C, the $Li_{1.10}Ni_{0.30}Co_{0.30}Mn_{0.40}O_2$ electrode exhibits excellent cycling performance with capacity retention ratio of about 90%, however, the other electrodes $Li_{1.00}Ni_{0.30}Co_{0.30}Mn_{0.40}O_2$, $Li_{1.05}Ni_{0.30}Co_{0.30}Mn_{0.40}O_2$, and $Li_{1.15}Ni_{0.30}Co_{0.30}Mn_{0.40}O_2$ show only 79, 66, and 40% capacity retention ratio, respectively. The obtained cycling results thus support that $Li_{1.10}Ni_{0.30}Co_{0.30}Mn_{0.4}O_2$ material has excellent high rate cycling, indicating possibility as a candidate of cathode material for high power lithium-ion batteries. Furthermore, the detrimental effect of the overlithiated phase ($Li_{1.15}Ni_{0.30}Co_{0.30}Mn_{0.40}O_2$) may be due to volume change. The extra Li more than appropriate amount may insert into the Li layer, causing an octahedral to tetrahedral coordination change for the Li ions in that layer, and the material expands. This results fragmentation of particle and loss of electrical contact and as a consequence the material with $x = 0.15$ fades more rapidly than the materials with $x = 0$, 0.05 and 0.10.

From the results obtained in this work, the influence of lithium content on the high rate performance can be explained as follows. Since Ni is in Ni^{2+} state in $LiNi_{0.30}Co_{0.30}Mn_{0.40}O_2$ material, it can accommodate considerable amount of lithium in the transition metal sites without disturbing the overall rhombohedra structure (R3-m) of the material. In $LiCoO_2$ and $LiNiO_2$ where Ni and Co ions exist as Co^{3+} and Ni^{3+} and these ions should be oxidized to Co^{4+} and Ni^{4+} to accept extra Li^+ in the transition metal site and this oxidation process is very difficult to occur under normal preparation conditions. However, in $LiNi_{0.30}Co_{0.30}Mn_{0.40}O_2$ where Ni exists as Ni^{2+}, addition of Li^+ in the transition metal site requires oxidation of Ni^{2+} to Ni^{3+}, which is a relatively easier process than oxidation of Ni^{3+} to Ni^{4+}. It has been reported if the lithium ions exist in the transition metal site in the layered structure containing Mn^{4+} as a major constituent, the Li^+ ions have a strong tendency to form a cation ordering with Mn^{4+} ions. This kind of phenomena has been observed and reported for Li_2MnO_3 or $Li[Li_{1/3}Mn_{2/3}]O_2$ and $Li[Ni_xLi_{1/3-2x/3}Mn_{2/3-x/3}]O_2$ materials [36,37]. The presence of the Li_2MnO_3 component in the composite structure also imparts quite interesting electrochemical properties to the electrode materials [31,32]. In the present work, since the lithium layer is fully occupied by 1Li in the layered structure of $Li_{1+x}Ni_{0.30}Co_{0.30}Mn_{0.40}O_2$, the excess lithium resides in the transition metal layer to form cation ordering with Mn ions, resulting in local Li_2MnO_3-like domains. In this work, the formation of Li_2MnO_3 was observed for lithium-excess $Li_{1+x}Ni_{0.30}Co_{0.30}Mn_{0.40}O_2$ from the XRD measurements (Fig. 1). Therefore, the excess lithium in $Li_{1+x}Ni_{0.30}Co_{0.30}Mn_{0.40}O_2$ is expected to affect the electronic structure by oxidizing Ni^{2+} ions as well as its crystallographic structure by forming a $Li_2MnO_3 \cdot (1-x)Li_{1+x}Ni_{0.30}Co_{0.30}Mn_{0.40}O_2$-type composite structure. The resultant electrochemical properties of the electrode materials are thus changed by the excess lithium content. In addition, the cation disorder for $Li_{1.10}Ni_{0.30}Co_{0.30}Mn_{0.40}O_2$ materials was found to be lower compared to other materials studied in this work. It can thus be concluded that significantly improved rate capability for lithium-excess $Li_{1.10}Ni_{0.30}Co_{0.30}Mn_{0.40}O_2$ was associated with two factors, (i) the enhanced structural stability by the formation of Li_2MnO_3 phase, and (ii) the enhanced lithium diffusivity due to the reduced Ni content in the Li layer.

4. Conclusions

Layered $Li_{1+x}Ni_{0.30}Co_{0.30}Mn_{0.40}O_2$ ($x = 0$, 0.05, 0.10, 0.15) materials were synthesized using citric acid assisted sol–gel process and the effect of the excess lithium on the crystal structure, and

electrochemical properties of the materials was investigated. The materials with higher Li content showed larger cation ordering peaks at 20–$25°2\theta_{CuK\alpha}$. These results indicate that Li_2MnO_3 or Li_2MnO_3-like phases are present in the materials with excess lithium. Rate capability and high rate cyleability were affected by lithium content. Among the materials studied in this work, $Li_{1.10}Ni_{0.30}Co_{0.30}Mn_{0.40}O_2$ cathode demonstrated the highest discharge capacity at different C-rates. In addition, upon extended cycling at high rates such as 1 and 8C, $Li_{1.10}Ni_{0.30}Co_{0.30}Mn_{0.40}O_2$ showed better capacity retention when compared to other materials with different lithium content. The improved high rate cycleability of $Li_{1.10}Ni_{0.30}Co_{0.30}Mn_{0.40}O_2$ cathode is ascribed to the improved structural stability due to the formation of appropriate amount of Li_2MnO_3-like domains in the transition metal layer and decreased cation (Li/Ni) disorder. Hence, it can be suggested that the $Li_{1.10}Ni_{0.30}Co_{0.30}Mn_{0.40}O_2$ material can be used as a possible cathode material for high power applications in response to an expanding need for advanced rechargeable lithium-ion batteries.

References

[1] B.L. Ellis, K.T. Lee, L.F. Nazar, Chem. Mater. 22 (2010) 691.
[2] P.G. Bruce, B. Scrosati, J.M. Tarascon, Angew. Chem. Int. Ed. 47 (2008) 2930.
[3] M.S. Whittingam, Chem. Rev. 104 (2004) 4271.
[4] J.M. Tarascon, M. Armond, Nature 414 (2001) 359.
[5] R.J. Brodd, K.R. Bullock, R.A. Leising, R.L. Middaugh, J.R. Miller, E. Takeuchic, J. Electrochem. Soc. 151 (3) (2004) K1.
[6] B. Ammundsen, J. Paulsen, Adv. Mater. 13 (2001) 943.
[7] B.J. Hwang, Y.W. Tsai, C.H. Chen, J. Mater. Chem. 13 (2003) 1962.
[8] B.J. Hwang, Y.W. Tsai, C.H. Chen, R. Santhanam, J. Mater. Chem. 13 (2003) 1962.
[9] S. Jouanneau, J.R. Dahn, Chem. Mater. 15 (2003) 495.
[10] J. Choi, A. Manthiram, J. Power Sources 162 (2006) 667.
[11] T. Ohzuku, Y. Makimura, Chem. Lett. 7 (2001) 642.
[12] B.J. Hwang, Y.W. Tsai, D. Carlier, G. Ceder, Chem. Mater. 15 (2003) 3676.
[13] R. Santhanam, B. Rambabu, J. Power Sources 195 (2010) 4313.
[14] S.H. Kang, K. Amine, J. Power Sources 146 (2005) 654.
[15] S.H. Park, S.W. Oh, Y.K. Sun, J. Power Sources 146 (2005) 622.
[16] Y.S. Meng, Y.W. Wu, B.J. Hwang, J. Electrochem. Soc. 151 (2004) A1134.
[17] Y.K. Sun, S.H. Kang, K. Amine, Mater. Res. Bull. 39 (2004) 819.
[18] N. Yabuuchi, T. Ohzuku, J. Power Sources 119–121 (2003) 171.
[19] K.M. Shaju, G.V. Subba Rao, B.V.R. Chowdari, Electrochim. Acta 48 (2002) 145.
[20] S.H. Na, H.S. Kim, S.I. Moon, Solid State Ionics 176 (2005) 313.
[21] D. Liu, Z. Wang, L. Chen, Electrochim. Acta 51 (2006) 4199.
[22] S.H. Hu, G.H. Cheng, M.Y. Cheng, B.J. Hwang, R. Santhanam, J. Power Sources 188 (2009) 564.
[23] H.S. Kim, Y. Kim, S.I. Kim, S.I. Moon, S.W. Martin, J. Power Sources 161 (2006) 623.
[24] Y.S. Kim, H.S. Kim, S.W. Martin, Electrochim. Acta 52 (2009) 1316.
[25] S.H. Kang, S.H. Park, C.S. Johnson, K. Amine, J. Electrochem. Soc. 154 (2007) A268.
[26] B.J. Hwang, R. Santhanam, D.G. Liu, J. Power Sources 97–98 (2001) 443.
[27] S.H. Kang, C.S. Johnson, J.T. Vaughey, K. Amine, M.M. Thackeray, J. Electrochem. Soc. 153 (2006) A1186.
[28] M.M. Thackeray, S.H. Kang, C.S. Johnson, J.T. Vaughey, S.A. Hackney, Electrochem. Commun. 8 (2006) 1531.
[29] C.S. Johnson, N. Li, J.T. Vaughey, S.A. Hackney, M.M. Thackeray, Electrochem. Commun. 7 (2005) 528.
[30] J.S. Kim, C.S. Johnson, J.T. Vaughey, M.M. Thackeray, S.A. Hackney, W. Yoon, C.P. Grey, Chem. Mater. 16 (2004) 1996.
[31] C.S. Johnson, J.-S. Kim, C. Lefief, N. Li, J.T. Vaughey, M.M. Thackeray, Electrochem. Commun. 6 (2004) 1085.
[32] M.M. Thackeray, C.S. Johnson, J.T. Vaughey, N. Li, S.A. Hackney, J. Mater. Chem. 15 (2005) 2257.

[33] Z. Chen, J.R. Dahn, Electrochem. Solid-State Lett. 5 (2002) A213.
[34] S.T. Myung, S. Komaba, K. Kurihara, K. Hosoya, N. Kumagai, Y.K. Sun, I. Nakai, M. Yonemura, T. Kamiyama, Chem. Mater. 18 (2006) 1658.
[35] K.S. Kang, Y.S. Meng, J. Greger, C.P. Grey, G. Ceder, Science 311 (2006) 977.
[36] V. Massarotti, M. Bini, D. Capsoni, A. Altomare, A.G.G. Moliterni, J. Appl. Crystallogr. 30 (1997) 123.
[37] Z. Lu, L.Y. Beaulieu, R.A. Donaberger, C.L. Thomas, J.R. Dahn, J. Electrochem. Soc. 149 (2002) A778.